

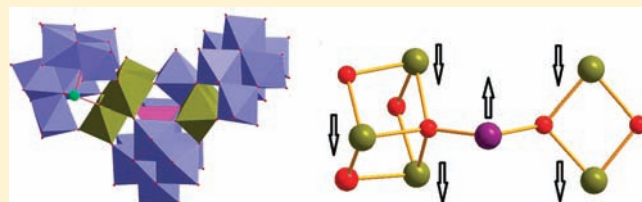
Three Banana-Shaped Arsenomolybdates Encapsulating a Hexanuclear Transition-Metal Central Magnetic Cluster: $[\text{As}^{\text{III}}_2\text{Fe}^{\text{III}}_5\text{MMo}_{22}\text{O}_{85}(\text{H}_2\text{O})]^{n-}$ ($\text{M} = \text{Fe}^{3+}$, $n = 14$; $\text{M} = \text{Ni}^{2+}$ and Mn^{2+} , $n = 15$)

Bin Liu, Lili Li, Yanping Zhang, Ying Ma, Huaming Hu, and Ganglin Xue*

Key Laboratory of Synthetic and Natural Functional Molecule Chemistry (Ministry of Education), Shaanxi Key Laboratory of Physico-Inorganic Chemistry, Department of Chemistry, Northwest University, Xi'an 710069, China

S Supporting Information

ABSTRACT: Three polyoxometalates encapsulating high-nuclearity magnetic clusters MFe_5 , $[\text{As}_2\text{MFe}_5\text{Mo}_{22}\text{O}_{85}(\text{H}_2\text{O})]^{n-}$ ($\text{M} = \text{Fe}^{3+}$, $n = 14$; $\text{M} = \text{Ni}^{2+}$ and Mn^{2+} , $n = 15$), were synthesized and characterized by single-crystal X-ray diffraction, elemental analysis, infrared spectroscopy, thermogravimetric analysis, and magnetism measurements. The polyanion $[\text{As}_2\text{MFe}_5\text{Mo}_{22}\text{O}_{85}(\text{H}_2\text{O})]^{n-}$ consists of a central $\text{MMo}_7\text{O}_{28}$ ($\text{M} = \text{Fe}^{3+}$, Ni^{2+} , and Mn^{2+}) fragment and two $\text{AsMo}_7\text{O}_{27}$ fragments linked together by two trimeric clusters, $\text{Fe}_2\text{MoO}(\mu_2\text{-O})_2$ and $\text{Fe}_3(\text{H}_2\text{O})$, to form a banana-shaped structure with C_1 symmetry. The $\text{MMo}_7\text{O}_{28}$ and $\text{AsMo}_7\text{O}_{27}$ units have a similar structure and can be considered as a monocapped hexavacant α -B-Keggin subunit with a central MO_4 group or a central $\text{As}^{\text{III}}\text{O}_3$ group. The polyoxometalates have a low absorption of $\nu(\text{Mo}-\text{O}_d)$ ($925\text{--}913\text{ cm}^{-1}$) because most of the Mo atoms in the polyanions have at least two longer $\text{Mo}-\text{O}_d$ bonds. The framework of the arsenomolybdates is stable before As_2O_3 escaping (ca. $300\text{ }^\circ\text{C}$). The analysis of magnetostructural correlations and magnetism measurements indicate the coexistence of ferro- and antiferromagnetic interactions, which give an overall ferromagnetic spin ground state in the compounds.



INTRODUCTION

Polyoxometalates (POMs) are a unique class of metal–oxygen cluster species with an enormous structural variety and a multitude of interesting properties.¹ Although POMs have been known for about 200 years, interest in this class of compounds is larger than ever before.² The sandwich-type complexes are one of the important subclasses, and the search for novel polyanions is predominantly driven by the catalytic and magnetic properties. Such compounds are usually composed of two trivalent Keggin or Dawson ligands (e.g., $\text{XM}_9\text{O}_{33\text{--}34}^{n-}$ ($\text{M} = \text{W}$ or Mo), $\text{X}'_2\text{W}_{15}\text{O}_{56}^{12-}$, $\text{X} = \text{P}$, As , Sb , Bi , Ge , Si , Co , Zn , etc.; $\text{X}' = \text{P}$, As) linked together by divalent or trivalent transition-metal ions varied from dinuclear to hexanuclear structures.³ Besides, several interesting double-sandwich or banana-shaped polyoxotungstates have been reported in recent years, such as $[\text{Co}_7(\text{H}_2\text{O})_2(\text{OH})_2\text{P}_2\text{W}_{25}\text{O}_{94}]^{16-}$,⁴ $[\text{Ni}_6\text{As}_3\text{W}_{24}\text{O}_{94}(\text{H}_2\text{O})_2]^{17-}$, and $[\text{Ni}_4\text{Mn}_2\text{P}_3\text{W}_{24}\text{O}_{94}(\text{H}_2\text{O})_2]^{17-}$,⁵ and $[\text{((MOH}_2)_2\text{M}_2\text{PW}_9\text{O}_{34})_2(\text{PW}_6\text{O}_{26})]^{17-}$ ($\text{M} = \text{Co}^{2+}$, Mn^{2+}),⁶ $[\text{((CoOH}_2)_2\text{Co}_2\text{GeW}_9\text{O}_{34})_2(\text{GeW}_6\text{O}_{26})]^{20-}$,⁷ and $[\text{Fe}_6\text{Ge}_3\text{W}_{24}\text{O}_{94}(\text{H}_2\text{O})_2]^{14-}$,⁸ all of which consist of two trivalent Keggin moieties XW_9O_{34} and a unique central XW_6O_{26} fragment linked via two transition metal M_3 clusters leading to a banana-shaped structure with C_{2v} symmetry. In 2009, the single molecule magnet based banana-shaped polyoxotungstate, $[\text{(Fe}_4\text{W}_9\text{O}_{34}(\text{H}_2\text{O}))_2(\text{FeW}_6\text{O}_{26})]^{19-}$, was reported by Mialane and co-workers.⁹ Compared with the extensive reports of sandwich-type polyoxotungstates, the molybdate analogues are very rare,^{10–12} due to the structural lability of lacunary heteropolymolybdate in aqueous

solution resulting in the difficulty in obtaining a sandwich-type molybdate. Here, we report a new family of polymolybdates, which are formulated as $(\text{NH}_4)_{12}\text{Cu}(\text{H}_2\text{O})_4[\text{As}_2\text{Fe}_6\text{Mo}_{22}\text{O}_{85}(\text{H}_2\text{O})] \cdot 20\text{H}_2\text{O}$ (1), $(\text{NH}_4)_{15}[\text{As}_2\text{NiFe}_5\text{Mo}_{22}\text{O}_{85}(\text{H}_2\text{O})] \cdot 17\text{H}_2\text{O}$ (2), and $(\text{NH}_4)_{14}\text{Mn}_{0.5}[\text{As}_2\text{MnFe}_5\text{Mo}_{22}\text{O}_{85}(\text{H}_2\text{O})] \cdot 22\text{H}_2\text{O}$ (3). To the best of our knowledge, these compounds represent the first example of double-sandwich molybdates. It is interesting that the magnetism measurements indicate the coexistence of ferro- and antiferromagnetic interactions, which give an overall ferromagnetic spin ground state in 1–3.

EXPERIMENTAL SECTION

General Methods and Materials. All chemicals were commercially purchased and used without further purification. Elemental analyses (H and N) were performed on a Perkin-Elmer 2400 CHN elemental analyzer; As, Mo, Fe, Cu, Mn, and Ni were analyzed on a IRIS Advantage ICP atomic emission spectrometer. IR spectra were recorded in the range of $400\text{--}4000\text{ cm}^{-1}$ on an EQUINOX55 FT/IR spectrophotometer using KBr pellets. TGA-DSC analyses were performed on a NETZSCH STA 449C TGA instrument in flowing N_2 with a heating rate of $10\text{ }^\circ\text{C} \cdot \text{min}^{-1}$. Magnetism measurements were performed on a Quantum Design MPMS SQUID magnetometer. The experimental susceptibilities were corrected for the diamagnetism of the constituent atoms (Pascal's tables).¹³

Received: July 4, 2011

Published: August 23, 2011

Table 1. Summary of Crystallographic Data for the Structures of 1–3

| | 1 | 2 | 3 |
|--|---|---|--|
| empirical formula | As ₂ CuFe ₆ H ₉₈ Mo ₂₂ N ₁₂ O ₁₁₀ | As ₂ Fe ₅ H ₉₆ Mo ₂₂ N ₁₅ NiO ₁₀₃ | As ₂ Fe ₅ H ₁₀₂ Mn _{1.5} Mo ₂₂ N ₁₄ O ₁₀₈ |
| <i>M</i> (g mol ⁻¹) | 4686.06 | 4553.40 | 4649.14 |
| cryst syst | triclinic | triclinic | triclinic |
| space group | <i>P</i> $\bar{1}$ | <i>P</i> $\bar{1}$ | <i>P</i> $\bar{1}$ |
| <i>a</i> (Å) | 16.1691(15) | 16.3842(11) | 12.664(5) |
| <i>b</i> (Å) | 18.3676(17) | 17.6856(11) | 16.216(7) |
| <i>c</i> (Å) | 20.8273(19) | 19.9638(13) | 26.974(11) |
| α (deg) | 96.626(2) | 93.3880 (10) | 100.818(7) |
| β (deg) | 105.4730(10) | 107.6070(10) | 92.650(7) |
| γ (deg) | 96.8410(10) | 99.4640 (10) | 103.425(6) |
| <i>V</i> , (Å ³) | 5848.4(9) | 5402.2(6) | 5269(4) |
| <i>Z</i> | 2 | 2 | 2 |
| temp (K) | 293(2) | 293(2) | 293(2) |
| <i>d</i> _{calcd} (g cm ⁻³) | 2.661 | 2.799 | 2.930 |
| GOF | 1.024 | 1.018 | 1.011 |
| <i>R</i> ₁ ^a (<i>I</i> > 2σ(<i>I</i>)) | 0.0585 | 0.0504 | 0.0837 |
| <i>wR</i> ₂ ^b (<i>I</i> > 2σ(<i>I</i>)) | 0.1932 | 0.1477 | 0.1901 |
| <i>R</i> ₁ ^a (all data) | 0.0846 | 0.0668 | 0.1698 |
| <i>wR</i> ₂ ^b (all data) | 0.2224 | 0.1661 | 0.2079 |

$$^a R_1 = [\sum |F_o| - |F_c|] / [\sum |F_c|]. \quad ^b wR_2 = \{[\sum w(F_o^2 - F_c^2)^2] / [\sum w(F_o^2)^2]\}^{1/2}.$$

(NH₄)₁₂Cu(H₂O)₄[As₂Fe₆Mo₂₂O₈₅(H₂O)]·20H₂O (**1**). The synthesis of **1** was accomplished by adding a solution of As₂O₃ (0.08 g, 0.4 mmol) dissolved in 6 M hydrochloric acid (2 mL) to a solution of (NH₄)₆Mo₇O₂₄·4H₂O (0.99 g, 0.8 mmol) dissolved in H₂O (10 mL). Then, 0.22 g of FeCl₃·6H₂O (0.8 mmol) was added, and the pH was adjusted to 6.0 by 3 M ammonium hydroxide. The resulting suspension was heated to about 90 °C, and a clear solution was formed. Solid CuCl₂·2H₂O (0.05 g, 0.3 mmol) was added to the hot solution, and the solution was heated for an additional 30 min. The hot solution was filtered and allowed to stand at ambient conditions. At this point, the pH was 6.2. Within several days, 0.45 g (yield 72% based on FeCl₃·6H₂O) of brown crystals were isolated. Elemental analysis calcd (%) for As₂CuFe₆H₉₈Mo₂₂N₁₂O₁₁₀: Mo, 45.0; As, 3.2; Fe, 7.2; Cu, 1.4; N, 3.6; H, 2.1. Found (%): Mo, 45.3; As, 3.2; Fe, 7.3; Cu, 1.5; N, 3.7; H, 2.1. IR for **1** (KBr, cm⁻¹): 925(m), 875(s), 825(m), 749(m), 675(s).

(NH₄)₁₅[As₂NiFe₅Mo₂₂O₈₅(H₂O)]·17H₂O (**2**). The synthetic procedure for **2** is similar to that of **1** except for using Ni(CH₃COO)₂·4H₂O (0.04 g, 0.16 mmol) instead of CuCl₂·2H₂O. Brown crystals (0.55 g) were isolated (yield 76% based on FeCl₃·6H₂O). Elemental analysis calcd (%) for As₂Fe₅H₉₆Mo₂₂N₁₅NiO₁₀₃: N, 4.6; H, 2.1; Fe, 6.1; Ni, 1.3; As, 3.3; Mo, 46.4. Found (%): N, 4.6; H, 2.3; Fe, 6.0; Ni, 1.3; As, 3.2; Mo, 46.9. IR for **2** (KBr, cm⁻¹): 925(m), 874(s), 825(m), 767(m), 670(s).

(NH₄)₁₄Mn_{0.5}[As₂MnFe₅Mo₂₂O₈₅(H₂O)]·22H₂O (**3**). The synthetic procedure for **3** is similar to that of **1** except for using MnCl₂·2H₂O (0.06 g, 0.4 mmol) instead of CuCl₂·2H₂O. Brown crystals (0.51 g, yield 69% based on FeCl₃·6H₂O) were isolated. Elemental analysis calcd (%) for As₂Fe₅H₁₀₂Mn_{1.5}Mo₂₂N₁₄O₁₀₈: Mo, 45.4; As, 3.2; Fe, 6.0; Mn, 1.8; N, 4.2; H, 2.2. Found (%): Mo, 46.1; As, 3.4; Fe, 6.3; Mn, 1.9; N, 4.3; H, 2.3. IR for **3** (KBr, cm⁻¹): 913(m), 877(s), 825(m), 771(m), 676(s).

X-Ray Crystallography. Intensity data were collected on a BRUKER SMART APEX II CCD diffractometer with Mo *K* α monochromated radiation ($\lambda = 0.71073$ Å) at 293 K. An empirical absorption correction was applied. The structures of **1–3** were solved by the direct method and refined by the Full-matrix least-squares on *F*² using the SHELXTL-97 software. All heavy atoms (As, Mo, Fe, Cu, Ni, and Mn) were refined with anisotropic displacement parameters, and the other atoms were refined isotropically. Hydrogen atoms were not included but

were included in the structure factor calculations. As usual for most of the polyoxometalates crystallized with amounts of water in which the counterions fill the cavities formed by the polyoxometalate arrangement, the crystal shows some disorder in the range of counterions and water molecules. For these hydrated ammonium salts, the data did not support discrimination between oxygen and nitrogen atoms, and the ammonium ions were modeled as oxygen atoms. Accordingly, the exact formula was determined by elemental analyses. A summary of the crystallographic data and structure refinement for compounds **1–3** is given in Table 1. Further details of the crystal structure investigation can be obtained from the Fachinformationszentrum Karlsruhe, 76344 Eggenstein-Leopoldshafen, Germany (fax, (49)7247-808-666; e-mail, crysdata@fiz-karlsruhe.de) on quoting the depository number CSD-419889, 423257, and 419891 for **1**, **2**, and **3**, respectively.

RESULTS AND DISCUSSION

Synthesis. Many factors can affect the isolation of final products, such as initial reactants, counter cations, pH values, reaction time, and temperature. In the synthesis of compounds **1–3**, pH value, counter cations, and temperature of the reaction system are of crucial importance for the formation of the final products. They were formed in similar conditions. For example, in the synthesis of **1**, the pH value should be carefully controlled between 5.5 and 6.5. When the pH value was lower than 5.5, [β -Mo₈O₂₆]⁴⁻ was the main product, and when the pH value was higher than 7.0, a large amount of unknown brown deposition was obtained. The temperature should be controlled at ca 90 °C; when the temperature was between 25 and 85 °C, the yellow sandwich-type heteropolymolybdate (NH₄)₁₂[Fe₂(AsMo₇O₂₇)₂]·16H₂O¹¹ was the main product, which can crystallize very quickly, even within several minutes. When the temperature rose to 90 °C, the sandwich dimer [Fe₂(AsMo₇O₂₇)₂]¹²⁻ would decompose gradually and transfer to [As₂Fe₆Mo₂₂O₈₅(H₂O)]¹⁴⁻ (**1a**). The addition of a small amount of Cu²⁺ is in favor of the isolation of **1a**; however, in the same reaction conditions using Ni²⁺ or Mn²⁺ instead of Cu²⁺, we

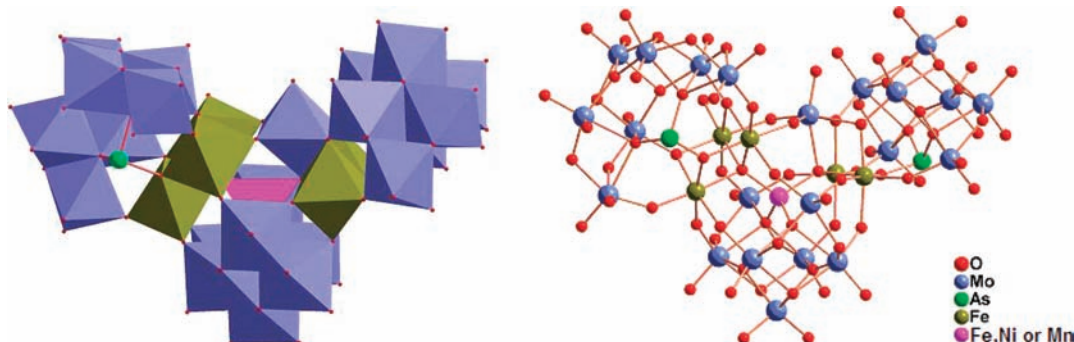


Figure 1. Combined polyhedral/ball-and-stick representation (left) and ball and stick representation (right) of double-sandwich polyoxomolybdates, $[\text{As}_2\text{MFe}_5\text{Mo}_{22}\text{O}_{85}(\text{H}_2\text{O})]^{n-}$ ($\text{M} = \text{Fe}, \text{Ni}$ or Mn).

got 2 and 3 in which Fe^{3+} in the central $\text{MMo}_7\text{O}_{28}$ fragment was substituted by Ni^{2+} or Mn^{2+} . In the absence of any NH_4^+ cations, no double-sandwich polymolybdates were obtained, which suggests that the structure is stabilized by NH_4^+ ions.

Structural Description of the Polyanions. X-ray structural analysis revealed that the structures of the polyanions $[\text{As}^{\text{III}}_2\text{Fe}^{\text{III}}_6\text{Mo}_{22}\text{O}_{85}(\text{H}_2\text{O})]^{14-}$ (**1a**), $[\text{As}^{\text{III}}_2\text{Ni}^{\text{II}}\text{Fe}^{\text{III}}_5\text{Mo}_{22}\text{O}_{85}(\text{H}_2\text{O})]^{15-}$ (**2a**), and $[\text{As}^{\text{III}}_2\text{Mn}^{\text{II}}\text{Fe}^{\text{III}}_5\text{Mo}_{22}\text{O}_{85}(\text{H}_2\text{O})]^{15-}$ (**3a**) are isostructural (Figure 1); therefore, only the structure of **1a** is discussed here. The polyoxoanion **1a** consists of a central $\text{FeMo}_7\text{O}_{28}$ fragment and two external $\text{AsMo}_7\text{O}_{27}$ fragments linked together by two trimeric clusters, $\text{Fe}_2\text{MoO}(\mu_2\text{-O})_2$ and $\text{Fe}_3(\text{H}_2\text{O})$, to form a double-sandwich C-shaped structure with C_1 symmetry; therefore, it can be expressed as $\{[\text{AsMo}_7\text{O}_{27}][\text{Fe}_2\text{MoO}(\mu_2\text{-O})_2][\text{FeMo}_7\text{O}_{28}][\text{Fe}_3(\text{H}_2\text{O})][\text{AsMo}_7\text{O}_{27}]\}^{14-}$. The structure of **1a** is somewhat analogous to those of the double-sandwich polyoxotungstates reported in recent years, such as $[\text{Co}_7(\text{H}_2\text{O})_2(\text{OH})_2\text{P}_2\text{W}_{25}\text{O}_{94}]^{16-}$,⁴ $[\text{Ni}_6\text{As}_3\text{W}_{24}\text{O}_{94}(\text{H}_2\text{O})_2]^{17-}$ and $[\text{Ni}_4\text{Mn}_2\text{P}_3\text{W}_{24}\text{O}_{94}(\text{H}_2\text{O})_2]^{17-}$,⁵ and $[\text{((MOH}_2)_2\text{M}_2\text{PW}_9\text{O}_{34})_2(\text{PW}_6\text{O}_{26})]^{17-}$ ($\text{M} = \text{Co}^{2+}, \text{Mn}^{2+}$),⁶ $[\text{((CoOH}_2)_2\text{Co}_2\text{GeW}_9\text{O}_{34})_2(\text{GeW}_6\text{O}_{26})]^{20-}$,⁷ and $[\text{Fe}_6\text{Ge}_3\text{W}_{24}\text{O}_{94}(\text{H}_2\text{O})_2]^{14-}$,⁸ which consist of two trivalent Keggin moieties XW_9O_{34} and a unique central XW_6O_{26} fragment linked via two M_3 clusters leading to a banana-shaped structure with C_{2v} symmetry. In the polyanion, the central $\text{FeMo}_7\text{O}_{28}$ fragment and external $\text{AsMo}_7\text{O}_{27}$ fragment have a similar structure, and both of them can be viewed as a monocapped hexavacant B- α -Keggin subunit with a central FeO_4 group or a central $\text{As}^{\text{III}}\text{O}_3$ group. The polyoxoanion contains an interesting monocapped cinque-substituted β -Keggin $[\text{Fe}(\text{Fe}_5\text{Mo}_7)\text{O}_{41}(\text{H}_2\text{O})]$ subunit derived from α -Keggin $[\text{FeMo}_{12}\text{O}_{40}]^{5-}$ through rotating a Mo_3O_{13} trimer 60° , replacing five MoO_6 with FeO_6 octahedra, and then capping one MoO_6 octahedron between two Mo_3O_{13} trimers (Scheme 1). Therefore, there are alternative possibilities of rationalizing the structure of **1a**, and we can say that it is formed by the condensation of two $\text{AsMo}_7\text{O}_{27}$ fragments and a novel monocapped cinque-substituted β -Keggin bridging cluster $[\text{Fe}(\text{Fe}_5\text{Mo}_7)\text{O}_{41}(\text{H}_2\text{O})]$. There are two different coordination Fe atoms in the polyanion; the Fe–O distances of the five octahedrally coordinated iron centers are in the range of 1.907(9)–2.208(9) Å in which the distance of $\text{Fe}-\text{O}_w$ is 1.981(11) Å, and the Fe–O distances of the tetrahedral coordinated iron in the central $\text{FeMo}_7\text{O}_{28}$ fragment are in the range of 1.873(8)–1.904(8) Å, and the bond lengths and angles of the molybdenum-oxo frameworks are within the usual ranges. Valence bond summations of Fe atoms in the $\text{Fe}_5\text{Mo}_3\text{O}_{3-}(\text{H}_2\text{O})$ cluster are in the range of 2.78–3.05, and the average value

is 2.91, and that in the FeO_4 group is 2.50; those of As1 and As2 are 2.88 and 2.93, respectively, and those of Mo are in the range of 5.96–6.17, which suggests that the valency of all the atoms remains unchanged. Interestingly, the Fe^{3+} in the central $\text{FeMo}_7\text{O}_{28}$ fragment of **1a** can be replaced by Ni^{2+} or Mn^{2+} to form isostructural compounds **2a** or **3a**. The selective bond lengths of compounds **1–3** are summarized in Tables 2 and 3.

FT-IR. IR spectra of the polyanions **1a–3a** are similar, and all of them have four characteristic vibration bands below 1000 cm^{-1} at 925–913, 877–874, 825, and 676–670 cm^{-1} , attributed to the characteristic vibrations of $\nu(\text{Mo}-\text{O}_d)$, $\nu(\text{O}_b-\text{Mo}-\text{O}_b)$, $\nu(\text{As}-\text{O}_a)$, and $\nu(\text{Mo}-\text{O}_c)$, respectively. It is worth noting that the polyoxometalates have a lower vibration band of $\nu(\text{Mo}-\text{O}_d)$ (925–913 cm^{-1}) compared with those ($\nu(\text{Mo}-\text{O}_d) = 950\text{ cm}^{-1}$) of other Keggin-type polyanions containing As^{III} as central heteroatoms¹⁰ because most of the Mo atoms in the polyanions have at least two longer Mo– O_d bonds rather than only one Mo– O_d bond.

Thermal Analyses. TGA-DSC curves (see Supporting Information) of **1–3** are very similar, and from the TGA-DSC curves, we can deduce that the thermal decomposition process is approximately divided into three steps. By taking compound $(\text{NH}_4)_{12}\text{Cu}(\text{H}_2\text{O})_4[\text{As}_2\text{Fe}_6\text{Mo}_{22}\text{O}_{85}(\text{H}_2\text{O})] \cdot 20\text{H}_2\text{O}$ (**1**) as an example, first, it gradually loses all water and NH_3 molecules at 25–310 °C. The total weight loss of 13.1% is consistent with the calculated value of 13.5%. Then, the weight loss of 4.3% (calcd 4.2%) from 310 to 410 °C is ascribed to the escaping of As_2O_3 . The last stage is the decomposition of the Mo–Fe–O framework structure, and the final product should be the mixed metal oxides $3\text{Fe}_2\text{O}_3 + \text{CuO} + 22\text{MoO}_3$, and the observed total weight loss of 19.6% can compare with the calculated value of 20.5%, accompanying a remarkable exothermal peak at around 456 °C.

Magnetic Properties. The magnetic properties of **1–3** were measured at a field of 0.1 T over the range 1.8–300 K. The $\chi_M T$ and χ_M^{-1} plots of **1–3** are shown in Figure 2. The experimental $\chi_M T$ values of **1–3** (CuFe_6 , NiFe_5 , and $\text{Mn}_{1.5}\text{Fe}_5$) at room temperature are 26.46, 23.73, and 26.64 emu K mol^{-1} , respectively, which correspond to the expected values of 26.62 emu K mol^{-1} for the total spin-only value for six Fe^{3+} ions ($s = 5/2, g = 2.0$) and one Cu^{2+} ions ($s = 1/2, g = 2.0$) for **1**, 22.87 emu K mol^{-1} for the total spin-only value for five Fe^{3+} ions ($s = 5/2, g = 2.0$) and one Ni^{2+} ions ($s = 1, g = 2.0$) for **2**, and 28.44 emu K mol^{-1} for the total spin-only value for five Fe^{3+} ions ($s = 5/2, g = 2.0$) and 1.5 Mn^{2+} ions ($s = 5/2, g = 2.0$) for **3**. The $\chi_M T$ values increase from ambient temperature down to 14.0, 14.0, and 18.0 K with a maximum of 55.4, 51.4, and 50.0 emu K mol^{-1} , respectively, then decrease sharply to 48.7, 49.8, and

Scheme 1. Derivation of Monocapped Cinque-Substituted β -Keggin $[M(\text{Fe}_5\text{Mo}_7)\text{O}_{41}(\text{H}_2\text{O})]$ ($M = \text{Fe}, \text{Ni}$ or Mn) in the Double-Sandwich Polyoxomolybdates

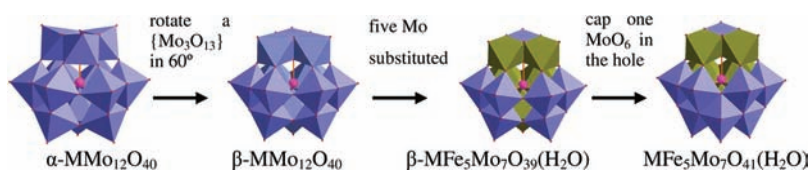


Table 2. Bond Lengths of $\text{Fe}_{\text{octa}}-\text{O}$ and $M_{\text{tetra}}-\text{O}$ and Bond Angles of $\text{Fe}_{\text{oct}}-\text{O}-\text{Fe}_{\text{oct}}$ and $\text{Fe}_{\text{oct}}-\text{O}-M_{\text{tetra}}$ in 1–3

| cmpds | $\text{Fe}_{\text{octa}}-\text{O}$ | | $M_{\text{tetra}}-\text{O}$ | | $\text{Fe}_{\text{oct}}-\text{O}-\text{Fe}_{\text{oct}}$ | | $\text{Fe}_{\text{oct}}-\text{O}-M_{\text{tetra}}$ | |
|-------|------------------------------------|-------|-----------------------------|-------|--|-------|--|--------|
| | average | | average | | average | | average | |
| 1 | 1.907–2.208 | 2.027 | 1.873–1.904 | 1.887 | 96.6–101.6 | 98.85 | 116.3–122.0 | 119.8 |
| 2 | 1.936–2.087 | 2.021 | 1.861–1.894 | 1.875 | 96.4–101.6 | 98.54 | 118.0–121.3 | 119.8 |
| 3 | 1.926–2.167 | 2.040 | 1.828–1.898 | 1.865 | 96.4–100.7 | 98.70 | 115.6–123.8 | 119.61 |

Table 3. Bond Lengths of $\text{Mo}-\text{O}$ and $\text{As}-\text{O}$ in 1–3

| cmpds | Mo_4-O | | Mo_6-O | | Mo_c-O | | $\text{As}-\text{O}$ | |
|-------|------------------------|-------|------------------------|-------|------------------------|-------|----------------------|-------|
| | average | | average | | average | | average | |
| 1 | 1.671–1.785 | 1.720 | 1.788–2.200 | 1.981 | 2.202–2.475 | 2.300 | 1.772–1.826 | 1.801 |
| 2 | 1.695–1.790 | 1.729 | 1.79–2.166 | 1.926 | 2.06–2.495 | 2.259 | 1.771–1.816 | 1.800 |
| 3 | 1.658–1.795 | 1.723 | 1.80–2.134 | 1.941 | 2.086–2.377 | 2.253 | 1.772–1.882 | 1.802 |

42.3 emu K mol^{-1} at 2 K for 1–3. The increase of $\chi_M T$ indicates the presence of dominant ferromagnetic interactions among magnetic centers, and the low-temperature drop may be attributed to secondary effects, such as zero-field splitting (ZFS) and/or intermolecular antiferromagnetic interactions.¹⁴ The temperature dependence of the reciprocal susceptibilities ($1/\chi_M$) during 300–100 K obeys the Curie–Weiss law with $C = 22.18 \text{ emu K mol}^{-1}$ and $\theta = 47.3 \text{ K}$ for 1, $C = 19.47 \text{ emu K mol}^{-1}$ and $\theta = 54.1 \text{ K}$ for 2, and $C = 22.92 \text{ emu K mol}^{-1}$ and $\theta = 40.3 \text{ K}$ for 3, respectively, which supports the presence of the overall ferromagnetic coupling among magnetic centers.

The double-sandwich POMs contain a six magnetic center cluster $M\text{Fe}^{\text{III}}_5$ ($M = \text{Fe}^{3+}, \text{Ni}^{2+},$ and Mn^{2+}), which represents a new type of magnetic core, and to the best of our knowledge, there are no hexanuclear $M\text{Fe}^{\text{III}}_5$ complexes relevant to 1–3 for which both the structural and the magnetic data have been reported. Considering that the determination of the magnetic exchange parameters by direct diagonalization of the adapted Heisenberg–Dirac–Van Vleck Hamiltonian is very difficult given the size of the matrices involved (ca. $10^6 \times 10^6$), and the analysis of the experimental magnetic susceptibility data using all of the spin states is an enormous task to undertake, and beyond the scope of the present undertaking, we focused our study on the determination of the nature of the spin ground state.

The multiplicity of the ground state in the $M\text{Fe}^{\text{III}}_5\text{O}_6$ ($M = \text{Fe}^{3+}, \text{Ni}^{2+},$ and Mn^{2+}) core can be rationalized in terms of magnetostructural correlations. It is well-known that for oxo-bridged high-spin Fe^{III} compounds, small $\text{Fe}-\text{O}$ bond lengths and large $\text{Fe}-\text{O}-\text{Fe}$ angles lead to large antiferromagnetic interactions.¹⁵ In approximation, the two contrary couplings are consistent with the

change in $M-\text{O}-M$ bridging angles in the $M\text{Fe}_5\text{O}_6$ core (shown in Figure 3): (a) antiferromagnetic coupling between the tetrahedrally coordinated M and the octahedrally coordinated Fe^{III} centers through one μ -oxo group with the angles of $M-\text{O}-\text{Fe}$ in the range of $115.6(6)^\circ$ – $123.8(6)^\circ$ and (b) ferromagnetic coupling between the octahedrally coordinated Fe^{III} centers with the angles in the range of $96.4(7)^\circ$ – $101.6(6)^\circ$ and an average of 98.8° .

The curves $M(H)$ data of 1–3 at 2.0 K are shown in Figure 4. These curves saturate at the value $M = 17.9 N\beta$ for 1, $M = 21.6 N\beta$ for 2, and $M = 19.4 N\beta$ for 3, where N is Avogadro's number and β is the Bohr magneton, which can be compared with the suggested spin alignments in the $M\text{Fe}_5\text{O}_6$ ($M = \text{Fe}^{3+}, \text{Ni}^{2+},$ or Mn^{2+}) core (Figure 3); $S = 10$ ground state for 1, $S = 10.5$ ground state for 2, and $S = 10$ ground state for 3. It is worth noting that the maximum $\chi_M T$ of 55.4, 51.4, and 50.0 emu K mol^{-1} for 1–3 (as shown in Figure 2) is a little lower than those of the suggested spin alignments. This phenomenon is possibly due to the presence of a positive zero field splitting or an orbital momentum in the ground states preventing the simple description, as the total spin is no longer a good quantum number,¹⁶ and besides, the outside coordinating metal-ions and/or intermolecular antiferromagnetic interaction cannot be excluded as well. It is interesting that all of the reported multi-iron POMs exhibit diamagnetic ground states^{11,17} with the $M-\text{O}-M$ bridging angles in the range of 86 – 139° , except those containing tetrahedrally coordinated Fe^{III} SMM based POMs [$(\text{Fe}_4\text{W}_9\text{O}_{34}(\text{H}_2\text{O}))_2(\text{FeW}_6\text{O}_{26})$]¹⁹ and [$\text{Fe}_4(\text{H}_2\text{O})_2(\text{FeWO}_3)_2$]¹⁰ with $S = 7.5$ and $S = 5$ ground states, respectively,^{9,18} in which the $\text{Fe}_{\text{tet}}-\text{Fe}_{\text{oct}}$ interactions are antiferromagnetic and the $\text{Fe}_{\text{oct}}-\text{Fe}_{\text{oct}}$ interactions are ferromagnetic; therefore, the tetrahedrally coordinated metal ion in the central fragment of the polyanion plays an important role in reducing the $\text{Fe}_{\text{oct}}-\text{O}-\text{Fe}_{\text{oct}}$

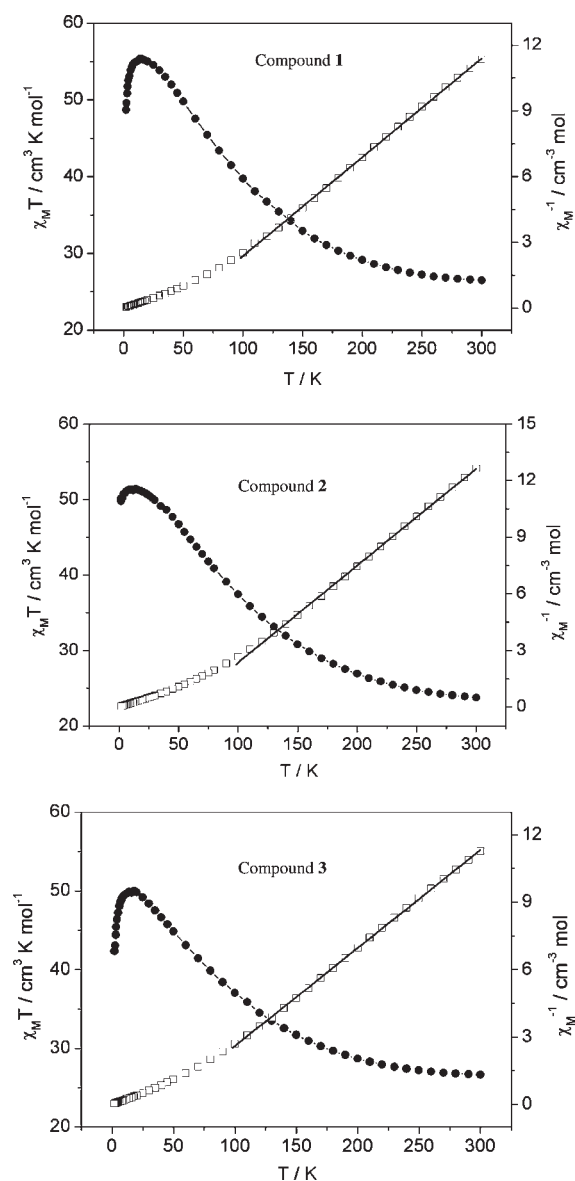


Figure 2. χ_M^{-1} and $\chi_M T$ plots for polycrystalline samples of 1–3 at a 1 kOe applied field.

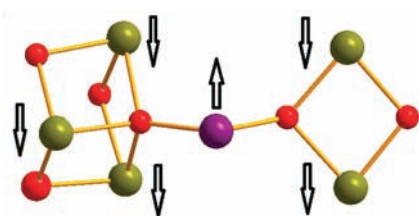


Figure 3. Possible spin alignments in the $M\text{Fe}_5\text{O}_6$ ($M = \text{Fe}^{3+}$, Ni^{2+} , or Mn^{2+}) core (O, red balls; Fe, yellow-brown balls; and M, purple ball) suggesting the ground state is $S = 10$ for 1, $S = 10.5$ for 2 and $S = 10$ for 3.

angle and results in ferromagnetic coupling between the octahedrally coordinated Fe^{III} centers. It is worth mentioning that no out-of-phase ac susceptibility (χ'') has been detected above 1.8 K (Figure S7 in the Supporting Information) for 1–3.

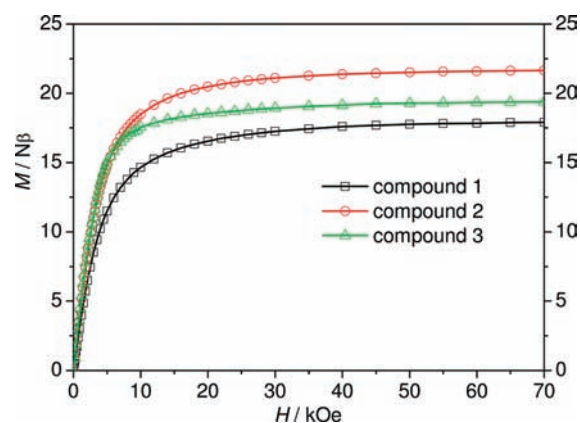


Figure 4. $M(H)$ data for polycrystalline samples of 1–3 at 2.0 K.

CONCLUSIONS

We have prepared three new polyoxometalates encapsulating hexanuclear transition-metal clusters, $[\text{As}_2\text{MFe}_5\text{Mo}_{22}\text{O}_{85}(\text{H}_2\text{O})]^{n-}$ ($M = \text{Fe}^{3+}$, $n = 14$; $M = \text{Ni}^{2+}$ and Mn^{2+} , $n = 15$), and the magnetic cluster MFe_5 represents a new type of magnetic core for which both the structural and the magnetic data have not yet been reported. The tetrahedral coordinated metal ion in the central fragment of the polyanions plays an important role in reducing the $\text{Fe}_{\text{oct}}-\text{O}-\text{Fe}_{\text{oct}}$ angle and resulting in ferromagnetic coupling between octahedrally coordinated Fe^{III} centers, and the overall ferromagnetic interactions are dominant in the clusters despite antiferromagnetic coupling between the tetrahedral coordinated M and the octahedrally coordinated Fe^{III} centers. One or more of the transition-metal ions encapsulated in the POMs fragments could be expected to be replaced by other transition-metal ions, thus opening the way for further theoretical and practical developments.

ASSOCIATED CONTENT

S Supporting Information. FT-IR spectra, TGA-DSC curves, χ' and χ'' plots for polycrystalline samples as well as crystallographic data in CIF format for compounds 1–3. This material is available free of charge via the Internet at <http://pubs.acs.org>.

AUTHOR INFORMATION

Corresponding Author

*E-mail: xglin707@163.com.

ACKNOWLEDGMENT

This research was supported by the National Natural Science Foundation of China (20973133), the Natural Science Foundation of Shaanxi Province (No. 2009JQ7010), and the Education Commission of Shaanxi Province (No. 09JK761).

REFERENCES

- (1) Pope, M. T. *Heteropoly and Isopoly Oxometalates*; Springer-Verlag: Berlin, Germany, 1983.
- (2) (a) Hill, C. L. *Chem. Rev.* **1998**, *98*, special thematic issue. (b) *Polyoxometalate Chemistry: From Topology via Self-Assembly to Applications*; Pope, M. T., Müller, A., Eds.; Kluwer: Dordrecht, The Netherlands, 2001. (c) *Polyoxometalate Chemistry for Nanocomposite Design*; Pope, M. T., Yamase, T., Eds.; Kluwer: Dordrecht, The Netherlands, 2001.

Netherlands, 2002. (d) Mizuno, N.; Yamaguchi, K.; Kamata, K. *Coord. Chem. Rev.* **2005**, *249*, 1944.

(3) Some examples of sandwich-type polyoxotungstates: (a) Neumann, R.; Khenkin, A. M. *Inorg. Chem.* **1995**, *34*, 5753. (b) Xin, F.; Pope, M. T. *Inorg. Chem.* **1996**, *35*, 5693. (c) Clemente-Juan, J. M.; Coronado, E.; Galán-Mascaros, J. R.; Gomez-Garcia, C. J. *Inorg. Chem.* **1999**, *38*, 55. (d) Zhang, X.; Anderson, T. M.; Chen, Q.; Hill, C. L. *Inorg. Chem.* **2001**, *40*, 418. (e) Anderson, T. M.; Hardcastle, K. I.; Okun, N.; Hill, C. L. *Inorg. Chem.* **2001**, *40*, 6418–6425. (f) Ruhlmann, L.; Canny, J.; Contant, R.; Thouvenot, R. *Inorg. Chem.* **2002**, *41*, 3811. (g) Kortz, U.; Nellutla, S.; Stowe, A. C.; N. Dalal, S.; Rauwald, U.; Danquah, W.; Ravot, D. *Inorg. Chem.* **2004**, *43*, 2308. (h) Belai, N.; Pope, M. T. *Chem. Commun.* **2005**, 5760. (i) Clemente-Juan, J. M.; Coronado, E.; Gaita-Arino, A.; Gimenez-Saiz, C.; Gudel, H.-U.; Sieber, A.; Bircher, R.; Mutka, H. *Inorg. Chem.* **2005**, *44*, 3389. (j) Yamase, T.; Fukaya, K.; Nojiri, H.; Ohshima, Y. *Inorg. Chem.* **2006**, *45*, 7698. (k) Zhang, Z.; Qi, Y.; Qin, C.; Li, Y.; Wang, E.; Wang, X.; Su, Z.; Xu, L. *Inorg. Chem.* **2007**, *46*, 8162. (l) Zheng, S.-T.; Yuan, D.-Q.; Zhang, J.; Yang, G.-Y. *Inorg. Chem.* **2007**, *46*, 4569. (m) Liu, Y.; Liu, B.; Xue, G.; Hu, H.; Fu, F.; Wang, J. *Dalton Trans.* **2007**, 3634. (n) Zhao, J.-W.; Zhang, J.; Zheng, S.-T.; Yang, G.-Y. *Chem. Commun.* **2008**, 570. (o) Nsouli, N. H.; Ismail, A. H.; Helgadottir, I. S.; Dickman, M. H.; Clemente-Juan, J. M.; Kortz, U. *Inorg. Chem.* **2009**, *48*, 5884. (p) Hou, Y.; Xu, L.; Cichon, M. J.; Lense, S.; Hardcastle, K. I.; Hill, C. L. *Inorg. Chem.* **2010**, *49*, 4125. (q) Reinoso, S.; Galán-Mascaros, J. R. *Inorg. Chem.* **2010**, *49*, 377.

(4) Borrás-Almenar, J. J.; Clemente-Juan, J. M.; Clemente-Leon, M.; Coronado, E.; Galán-Mascaros, J. R.; Gomez-Garcia, C. J. *Polyoxometalate Chemistry: From Topology Via Self-Assembly to Applications*; Pope, M. T., Müller, A., Eds.; Kluwer: Dordrecht, The Netherlands, 2001; p 231.

(5) Mbomekalle, I. M.; Keita, B.; Nierlich, M.; Kortz, U.; Berthet, P.; Nadjo, L. *Inorg. Chem.* **2003**, *42*, 5143.

(6) Ritorto, M. D.; Anderson, T. M.; Neiwert, W. A.; Hill, C. L. *Inorg. Chem.* **2004**, *43*, 44.

(7) Tong, R.; Chen, L.; Liu, Y.; Liu, B.; Xue, G.; Hu, H.; Fu, F.; Wang, J. *Inorg. Chem. Commun.* **2010**, *13*, 98.

(8) Li, B.; Zhao, J.-W.; Zheng, S.-T.; Yang, G.-Y. *Inorg. Chem. Commun.* **2009**, *12*, 69.

(9) Compain, J.-D.; Mialane, P.; Dolbecq, A.; Mbomekalle, I. M.; Marrot, J.; Sécheresse, F.; Rivière, E.; Rogez, G.; Wernsdorfer, W. *Angew. Chem., Int. Ed.* **2009**, *48*, 3077.

(10) Müller, A.; Krickmeyer, E.; Dillinger, S.; Meyer, J.; Bögge, J. H.; Stämmler, A. *Angew. Chem., Int. Ed.* **1996**, *35*, 171.

(11) (a) Li, L.; Shen, Q.; Xue, G.; Xu, H.; Hu, H.; Fu, F.; Wang, J. *Dalton Trans.* **2008**, 5698. (b) Xu, H.; Li, L.; Liu, B.; Xue, G.; Hu, H.; Fu, F.; Wang, J. *Inorg. Chem.* **2009**, *48*, 10275.

(12) (a) Fukushima, H. F.; Kobayashi, A.; Sasaki, Y. *Acta Crystallogr., Sect. B: Struct. Sci.* **1981**, *37*, 1613. (b) Dang, D.; Bai, Y.; He, C.; Wang, J.; Duan, C.; Niu, J. *Inorg. Chem.* **2010**, *49*, 1280.

(13) Kahn, O. *Molecular Magnetism*; VCH Publishers: New York, 1993.

(14) (a) Serna, Z. E.; Lezama, L.; Urriaga, M. K.; Arriortua, M. I.; Barandika, M. G.; Cortés, R.; Rojo, T. *Angew. Chem., Int. Ed.* **2000**, *39*, 344. (b) King, P.; Clérac, R.; Wernsdorfer, W.; Anson, C. E.; Powell, A. K. *Dalton Trans.* **2004**, 2670. (c) Fondo, M.; Ocampo, N.; García-Deibe, A. M.; Vicente, R.; Corbella, M.; Bermejo, M. R.; Sanmartín, J. *Inorg. Chem.* **2006**, *45*, 255.

(15) Canana-Vilalta, C.; O'Brien, T. A.; Brechin, E. K.; Pink, M.; Davidson, E. R.; Christou, G. *Inorg. Chem.* **2004**, *43*, 5505.

(16) Clemente-Juan, J. M.; Coronado, E. *Coord. Chem. Rev.* **1999**, *193–195*, 361.

(17) (a) Mbomekalle, I. M.; Keita, B.; Nadjo, L.; Berthet, P.; Hardcastle, K. I.; Hill, C. L.; Anderson, T. M. *Inorg. Chem.* **2003**, *42*, 1163. (b) Keita, B.; Mbomekalle, I. M.; Lu, Y. W.; Nadjo, L.; Berthet, P.; Anderson, T. M.; Hill, C. L. *Eur. J. Inorg. Chem.* **2004**, *2004*, 3462. (c) Bi, L.-H.; Kortz, U.; Nellutla, S.; Stowe, A. C.; van Tol, J.; Dalal, N. S.; Keita, B.; Nadjo, L. *Inorg. Chem.* **2005**, *44*, 896. (d) Godin, B.; Chen, Y.-G.; Vaissermann, J.; Ruhlmann, L.; Verdager, M.; Gouzerh, P. *Angew. Chem., Int. Ed.* **2005**, *44*, 3072. (e) Zhao, J.-W.; Zhang, J.; Zheng, S.-T.; Yang, G.-Y. *Inorg. Chem.* **2007**, *46*, 10944. (f) Nsouli, N. H.; Mal, S. S.;

Dickman, M. H.; Kortz, U.; Keita, B.; Nadjo, L.; Clemente-Juan, J. M. *Inorg. Chem.* **2007**, *46*, 8763. (g) Dolbecq, A.; Compain, J.-D.; Mialane, P.; Marrot, J.; Rivière, E.; Sécheresse, F. *Inorg. Chem.* **2008**, *47*, 3371. (h) Pichon, C.; Dolbecq, A.; Mialane, P.; Marrot, J.; Rivière, E.; Goral, M.; Zynek, M.; McCormac, T.; Borshch, S. A.; Zueva, E.; Sécheresse, F. *Chem.—Eur. J.* **2008**, *14*, 3189.

(18) Giusti, A.; Charron, G.; Mazerat, S.; Compain, J.-D.; Mialane, P.; Dolbecq, A.; Rivière, E.; Wernsdorfer, W.; Biboum, R. N.; Keita, B.; Nadjo, L.; Filoramo, A.; Bourgoin, J.-P.; Mallah, T. *Angew. Chem., Int. Ed.* **2009**, *48*, 4949.